Inorg. Chem. **2003**, *42*, 3978–3980

Salt-Inclusion Synthesis of $Ba_2MnSi_2O_7Cl$. A Fresnoite-Type Polar Framework Containing the Acentric $[Si_2O_7]^{6-}$ Polyanion in the Anti-ReO_3 Type $[(Ba_2Mn)Cl]^{6+}$ Cage

Xunhua Mo and Shiou-Jyh Hwu*

Department of Chemistry, Clemson University, Clemson, South Carolina 29634-0973

Received February 27, 2003

A novel non-centrosymmetric (NCS) solid, $Ba_2Mn(Si_2O_7)Cl$ (CU-13), was isolated via high-temperature, salt-inclusion reactions. This manganese(III) silicate chloride adopts the *fresnoite* structure exhibiting pseudo-one-dimensional channels in which the Ba^{2+} cations reside. The framework can be viewed alternatively as made of a fascinating anti-ReO_3 type $(Ba_2Mn)Cl$ lattice centered on the acentric Si_2O_7 unit. This new compound crystallizes in one of the 10 NCS polar crystal classes, 4*mm* (C_{4v}), which is cooperatively attributed to the MnO_4Cl_2 tetragonal distortion and the oriented Si_2O_7 polyhedral unit. This discovery once again demonstrates the utility of salt inclusion with the formation of NCS frameworks.

Non-centrosymmetric (NCS) synthesis has attracted constant attention for its importance in materials design for nonlinear applications.[1] Some recent synthesis strategies for NCS inorganic solids include using chiral organic molecules or metal complexes as templating agents,[2] employing enantiopure metal−organic clusters as secondary building blocks,[3] acentric packing of helical chain via directed metal−ligand−metal linkages,[4] incorporating acentric polyanions to stereochemically enforce acentricity of the bulk,[5] and incorporating cations with nonbonding electron pairs or d^0 transition metal cations showing cooperative second-order, Jahn−Teller (SOJT) distortions.[6]

Our recent discoveries of salt-inclusion solids have shed new light on the exploration of special frameworks via composite (hybrid) solids of mixed ionic and covalent sublattices.[7] This new class of open-framework solids has revealed the propensity of the incorporated halide salt to direct the porous structure, e.g., $A_2M_3(X_2O_7)_2{\cdot}$(salt) (A = K, Rb, Cs; M = Mn, Cu, X = P, As) (CU-2),[7e] $Na_2Cs_2Cu_3(P_2O_7)_2Cl_2$ (CU-4),[7d] $Cs_2Cu_7(P_2O_7)_4{\cdot}6CsCl$ (CU-9), $Cs_2Cu_5(P_2O_7)_3{\cdot}3CsCl$ (CU-11),[7a,b] and $CuPO_4{\cdot}BaCl$.[7g] It has been evident in these structures that the chlorine-centered secondary building unit (SBU), $ClA_{6-n}Cu_n$ (A = Cs, Ba; n = 1, 2), introduces the templating effect, including the acentricity, leading to the formation of NCS lattices. We have expanded the investigations into silicate systems due to the versatility of silicate-based acentric polyanions. Herein we report the fascinating barium manganese(III) silicate chloride $Ba_2MnSi_2O_7Cl$ that reveals the cooperative Jahn−Teller distortion and the utilities of polar anion and salt inclusion with the formation of the NCS lattice.

The crystals of $Ba_2Mn(Si_2O_7)Cl$ were grown in the molten $BaCl_2$/NaCl eutectic flux.[8] Single-crystal structure was

* Corresponding author. E-mail: shwu@clemson.edu.

(1) Some example literature and references therein: (a) Bein, T. *Curr. Opin. Solid State Mater. Sci.* **1999**, *4*, 85−96. (b) Keszler, D. A. *Curr. Opin. Solid State Mater. Sci.* **1999**, *4*, 155−162. (c) Yaghi, O. M.; Li, H.; Davis, C.; Richardson, D.; Groy, T. L. *Acc. Chem. Res.* **1998**, *31*, 474−484. (d) Marder, S. R.; Sohn, J. E.; Stucky, G. D. *Materials for Nonlinear Optics: Chemical Perspective*; ACS Symposium Series 455; American Chemical Society: Washington, DC, 1991.

(2) (a) Yu, J.; Wang, Y.; Shi, Z.; Xu, R. *Chem. Mater.* **2001**, *13*, 2972−2978. (b) Bruce, D.; Wilkinson, A. P.; White, M. G.; Bertrand, J. A. *J. Solid State Chem.* **1996**, *125*, 228−233. (c) Bruce, D.; Wilkinson, A. P.; White, M. G.; Bertrand, J. A. *J. Chem. Soc., Chem. Commun.* **1995**, 2059−2060.

(3) (a) Evans, O. R.; Lin, W. *Chem. Mater.* **2001**, *13*, 3009−3017. (b) Seo, J. S.; Whang, D.; Lee, H.; Jun, S.; Oh, J.; Jeon, Y.; Kim, K. *Nature* **2000**, *404*, 982−986. (c) Kepert, C. J.; Prior, T. J.; Rosseinsky, M. J. *J. Am. Chem. Soc.* **2000**, *122*, 5158−5168.

(4) (a) Maggard, P. A.; Stern, C. L.; Poeppelmeier, K. R. *J. Am. Chem. Soc.* **2001**, *123*, 7742−7743. (b) Maggard, P. A.; Kopf, A. L.; Stern, C. L.; Poeppelmeier, K. R.; OK, K. M.; Halasyamani, P. S. *Inorg. Chem.* **2002**, *41*, 4852−4858.

(5) (a) Norquist, A. J.; Heier, K. R.; Halasyamani, P. S.; Stern, C. L.; Poeppelmeier, K. R. *Inorg. Chem.* **2001**, *40*, 2015−2019. (b) Sykora, R. E.; Ok, K. M.; Halasyamani, P. S.; Albrecht-Schmitt, T. E. *J. Am. Chem. Soc.* **2002**, *124*, 1951−1957.

(6) (a) Shehee, T. C.; Sykora, R. E.; Ok, K. M.; Halasyamani, P. S.; Albrecht-Schmitt, T. E. *Inorg. Chem.* **2003**, *42*, 457−462. (b) Ok, K. M.; Goodey, J.; Broussard, J.; Halasyamani, P. S. *Chem. Mater.* **2002**, *14*, 3174−3180. (c) Porter, Y.; Bhuvanesh, N. S. P.; Halasyamani, P. S. *Inorg. Chem.* **2001**, *40*, 1172−1175. (d) Porter, Y.; Bhuvanesh, N. S. P.; Halasyamani, P. S. *Chem. Mater.* **2001**, *13*, 1910−1915. (e) Halasyamani, P. S.; O'Hare, D. *Chem. Mater.* **1998**, *10*, 646−649. (f) Halasyamani, P. S.; O'Hare, D. *Inorg. Chem.* **1997**, *36*, 6409−6412.

(7) (a) Huang, Q.; Hwu, S.-J. *Inorg. Chem.* **2003**, *42*, 655−657. (b) Huang, Q.; Ulutagay-Kartin, M.; Mo, X.; Hwu, S.-J. *Mater. Res. Soc. Symp. Proc.* **2003**, *755*, DD12.4. (c) Hwu, S.-J.; Ulutagay-Kartin, M.; Clayhold, J. A.; Mackay, R.; Wardojo, T. A.; O'Connor, C. J.; Krawiec, M. *J. Am. Chem. Soc.* **2002**, *124*, 12404-12405. (d) Huang, Q.; Hwu, S.-J.; Mo, X. *Angew. Chem., Int. Ed.* **2001**, *40*, 1690−1693. (e) Huang, Q.; Ulutagay, M.; Michener, P. A.; Hwu, S.-J. *J. Am. Chem. Soc.* **1999**, *121*, 10323-10326. (f) Ulutagay, M.; Shimek, G. L,; Hwu, S.-J.; Taye, H. *Inorg. Chem.* **1998**, *37*, 1507−1512. (g) Etheredge, K. M. S.; Hwu, S.-J. *Inorg. Chem.* **1995**, *34*, 3123−3125.

10.1021/ic0342245 CCC: $25.00
Published on Web 05/30/2003

Table 1. Selected Crystal and Refinement Data for $Ba_2MnSi_2O_7Cl$

empirical formula	$Ba_2MnSi_2O_7Cl$
fw	533.25
space group, Z	$P4bm$ (No. 100), 2
T, °C	27
a, Å	8.494(1)
c, Å	5.403(1)
V, Å^3	389.8(1)
μ(Mo Kα), mm^{-1}	12.23
d_{calc}, g cm^{-3}	4.543
data/restraints/params	565/1/39
secondary extinction	0.0090(9)
final R1, wR2[a] [$I > 2\sigma(I)$], GOF	0.0164/0.0402/1.05

[a] $R = \sum||F_o| - |F_c||/\sum|F_o|$; $wR2 = [\sum w(|F_o| - |F_c|)^2/\sum w|F_o|^2]^{1/2}$; $w = 1/[\sigma^2(F_o^2) + (0.0286P)^2 + 1.07P]$, where $P = (F_o^2 + 2F_c^2)/3$.

Table 2. Atomic Coordinates and Isotropic Equivalent Displacement Parameters for $Ba_2MnSi_2O_7Cl$

atom	Wyckoff position	x	y	z	U_{eq} (Å^2)[a]
Ba	4c	−0.16971(2)	−0.66971(2)	−0.8165(1)	0.0097(1)
Mn	2a	0	0	−0.1994(2)	0.0075(2)
Si	4c	−0.1297(1)	−0.3703(1)	−0.2975(4)	0.0081(3)
Cl	2a	0	0	−0.6736(3)	0.0124(3)
O(1)	4c	−0.1289(3)	−0.3711(3)	−0.5929(7)	0.0112(7)
O(2)	2b	0	−0.5	−0.187(1)	0.0136(9)
O(3)	8d	−0.2071(3)	−0.9206(3)	−0.1624(5)	0.0154(5)

[a] Equivalent isotropic U defined as one-third of the trace of the orthogonalized $\mathbf{U}_{ij}$ tensor.

determined by X-ray diffraction methods.[9] The crystallographic data and atomic parameters are listed in Tables 1 and 2, respectively. The title compound crystallizes in one of the 10 NCS polar, nonchiral crystal classes, *4mm* (C_{4v}).[10] The reddish color of the compound is diagnostically approved, according to reported procedures,[11] by the UV−vis spectrum with absorption peaks at 2.30 eV (18 550 cm^{-1}) and 2.80 eV (22 580 cm^{-1}), as shown in Figure 1, due to the $^5B_{1g} \rightarrow {}^5E_g$ and $^5B_{1g} \rightarrow {}^5B_{2g}$ transitions, respectively.[12] The compound is otherwise a wide band gap semiconductor with the characteristic absorption edge above 3.20 eV.

As shown in Figure 2, the title compound exhibits pseudo-one-dimensional channel structures where Ba^{2+} cations reside. The channels reveal a pentagonal window made of

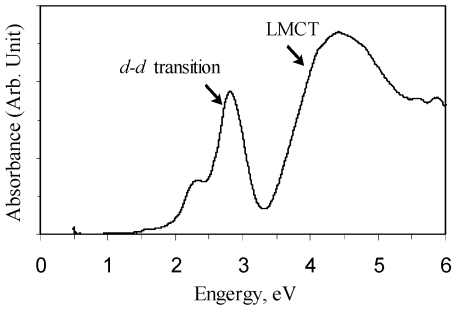

Figure 1. UV−vis spectrum of $Ba_2MnSi_2O_7Cl$.

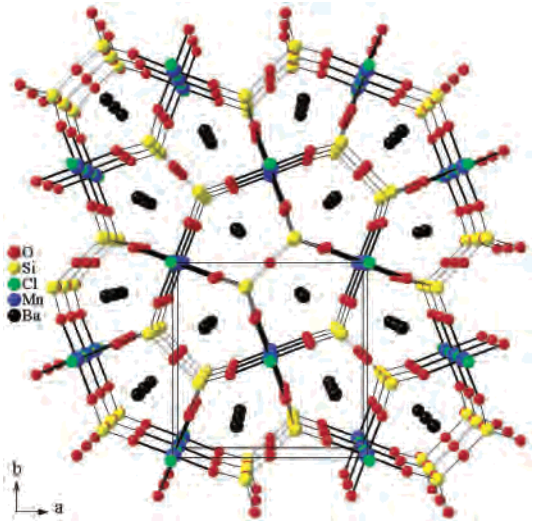

Figure 2. Perspective view of $Ba_2MnSi_2O_7Cl$ showing channel structures.

edges of the Si_2O_7 and MnO_4Cl_2 polyhedral units that share vertex oxygen atoms. The two symmetry planes along (220) and ($\bar{2}$20) intercept at the bridging oxygen, O(2), of the Si_2O_7 unit. The Ba^{2+} cations reside in these planes while the Cl^- anions are located between the Mn^{3+} cations leading to the linear chain of corner-shared MnO_4Cl_2 units along c. The latter adopts a tetragonal distortion giving rise to one short Mn−Cl bond, 2.562(2) Å, and one long Mn−Cl bond, 2.841(2) Å, which are significantly longer than 2.46 Å, the sum of Shannon crystal radii of six-coordinate Mn^{3+} (0.785 Å, high-spin) and Cl^- (1.67 Å).[13] The MnO_4 unit forms a square pyramid with four uniform Mn−O bonds, 1.895(3) Å, and a nearly perfect sum of ∠Mn−O−Mn angles, 357.4°. This tetragonal distortion, elongation along the Mn−Cl bonds, is intuitively attributed to the d^4 Mn^{3+} Jahn−Teller effect.

The extended framework consists of Mn−O−Si and Ba−Cl slabs alternately stacking along c, corresponding to Ti−O−Si and Ba−O slabs shown in the $Ba_2TiSi_2O_8$ fresnoite structure.[14] Figure 3 shows, in ORTEP drawings, a section of the neighboring slabs that are interlinked via the shorter Mn−Cl bond. The side view of the stacked slabs (Figure 3b) shows that the Ba−Cl layer is puckered, which is likely due to the lattice mismatching.[15] The Ba−Cl bond distances,

(8) Crystals of $Ba_2Mn(Si_2O_7)Cl$ were grown by employing eutectic $BaCl_2$/NaCl flux in a fused silica ampule under vacuum. Aldrich BaO (3 mmol, 97%), $BaCl_2$ (1 mmol, 99.9%), Mn_2O_3 (1 mmol, 99%), and SiO_2 (4 mmol, fused, 99.9%) were mixed and ground with flux (1:3 by weight) in a nitrogen-blanketed drybox. The mixture was heated to 900 °C and isothermed for 6 days, followed by slow cooling to 300 °C at 6 °C/h and then furnace cooling to room temperature. The reddish column crystals were retrieved upon washing off the salt with deionized water; ca. 90% yield, based on Mn_2O_3, was obtained.

(9) Data collection: on a four-circle Riguku AFC8 diffractometer equipped with a Mercury CCD area detector, Mo Kα ($\lambda = 0.71073$ Å) radiation, $T = 300$ K. The structure was solved by direct methods using the SHELXL-97 program and refined on F^2 by least-squares, full-matrix techniques. The final Fourier difference synthesis showed minimum and maximum peaks of −0.95 and +0.73 e/Å^3. The absolute configuration was determined on the basis of comparison using Friedel pairs. The chemical contents were confirmed by qualitative EDAX analysis. (a) Sheldrick, G. M. In *Crystallographic Computing 3*; Shledrick, G. M., Kruger, C., Goddard, R., Eds.; Oxford University Press: London, 1985; pp 175−189. (b) Sheldrick, G. M. In *SHELXTL, Version 6.1 Structure Determination Software Programs*; Bruker Analytical X-ray Systems Inc.: Madison, WI, 2001.

(10) Halasyamani, P. S.; Poeppelmeier, K. R. *Chem. Mater.* **1998**, *10*, 2753−2769.

(11) Ulutagay-Kartin, M.; Hwu, S.-J.; Clayhold, J. A. *Inorg. Chem.* **2003**, *42*, 2405−2409.

(12) Rodrígues, F.; Nuñez, P.; Marco de Lucas, M. C. *J. Solid State Chem.* **1994**, *110*, 370−383.

(13) Shannon, R. D. *Acta Crystallogr., Sect. A.* **1976**, *32*, 751−767.

(14) Moore, P. B.; Louisnathan, J. *Science* **1967**, *156*, 1361−1362.

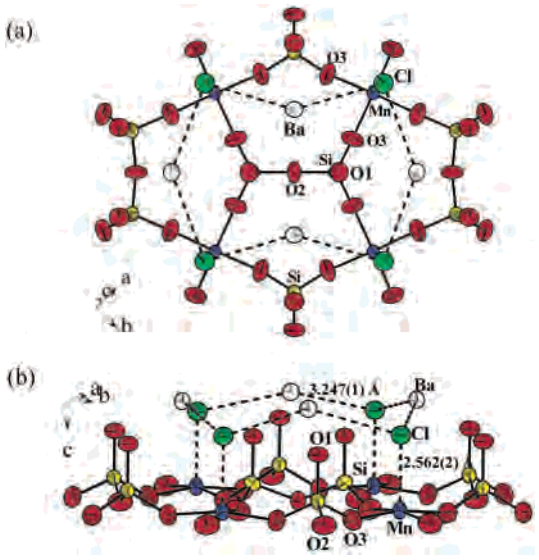

Figure 3. A section of the structure viewed (a) along *c* and (b) from the side showing the stacking of the Mn−Si−O and Ba−Cl slabs. The thermal ellipsoids were drawn at 95% probability.

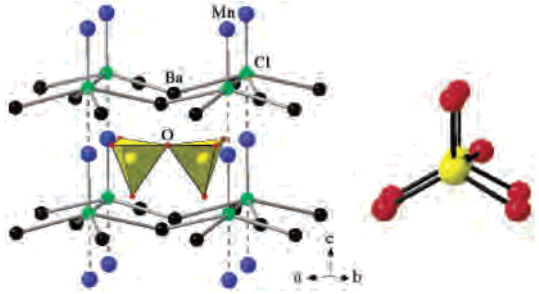

Figure 4. A cage view showing the Si_2O_7 unit residing in the center of the anti-ReO_3 type $(Ba_2Mn)Cl$ lattice (left). The Si_2O_7 unit is made of two corner-shared SiO_4 tetrahedra in an eclipsed configuration (right).

3.247(1) Å, are slightly shorter than 3.33 Å, the sum of Shannon radii.[13] It would be interesting to see if substituting Ba^{2+} with Sr^{2+} could affect the distortion and the nonlinear properties, including the negative thermal expansion behavior,[16] currently under investigation.

The polarity and, in turn, the bulk acentricity have been the most conspicuous structural features of interest in the title compound. The extended framework can be viewed as constructed by two SBUs: anti-ReO_3 type $(Ba_2Mn)Cl$ cage and Si_2O_7 pyrosilicate. As shown in Figure 4 (left), the distorted $(Ba_2Mn)Cl$ cage is made of corner-shared $ClBa_4Mn_2$, and the Si_2O_7 unit is caged in the center of this anti-ReO_3 lattice. The pyrosilicate unit (Figure 4, right) is formed by two corner-shared SiO_4 tetrahedra in an eclipsed configuration. The structure formula can thus be rewritten as $(Si_2O_7)@(Ba_2Mn)Cl$ ($\equiv Ba_2MnSi_2O_7Cl$). The preferred orientation with respect to the Si_2O_7 polar unit and the tetragonal elongation results in the bulk polarity along *c*.

The extended $(Ba_2Mn)Cl$ lattice (Figure 5) shows that the chlorine atoms are displaced (see the green circle in the

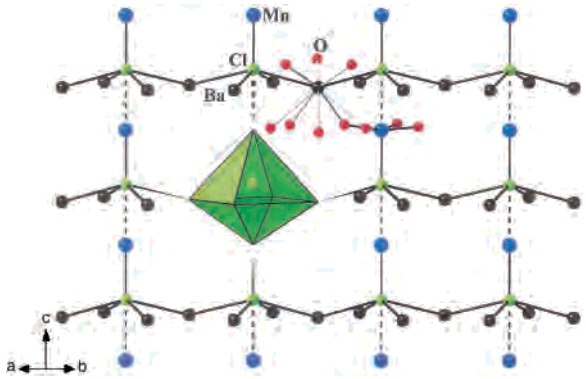

Figure 5. A slab of the $(Ba_2Mn)Cl$ lattice showing the origin of the polar lattice. The Mn−Cl linkages along *c* consist of alternating short (solid lines) and long (dotted lines) bonds giving rise to the distorted "Ba_4Mn_2" octahedra. The latter is shown, for clarity, by one Cl-centered octahedron in green. Selected Ba−O and Mn−O bonds are drawn to outline the respective coordination and connectivity.

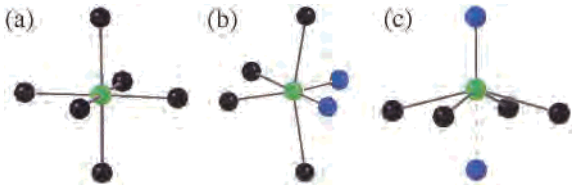

Figure 6. Coordination around chlorine in (a) NaCl, (b) CU-9 and CU-11, and (c) $Ba_2MnSi_2O_7Cl$. The electropositive cations are drawn in black and transition metal cations in blue.

highlighted $ClBa_4Mn_2$ octahedron) along the polar axis *c*. The barium cations adopt the BaO_8Cl_2 coordination, which is shown by Ba−O and Ba−Cl bonds, sharing edges with the square planar MnO_4 unit.

We have reported yet another example of a salt-inclusion solid showing the stuctural directing effect of the chlorine-centered $ClA_{6-n}M_n$ octahedral SBU, whose centricity can be varied via cation substitutions. The dication substitution ($n = 2$) in $ClNa_6$ (Figure 6a) can occur either in the cis positions (Figure 6b), as seen in the CU-9 and CU-11 structures (A = Cs, M = Cu),[7a,b] or in the trans (Figure 6c), as shown in CU-13 (A = Ba, M = Mn). It should be noted that the incorporation of acentric SBU is a necessary but not sufficient condition for bulk acentricity. In other words, the material can crystallize such that the distortions occur in an antiparallel manner, thus producing macroscopic centricity. The formation of $Ba_2MnSi_2O_7Cl$ demonstrates the utilities of polar anion, Jahn−Teller distortion and once again the salt inclusion with the formation of NCS lattice.

Acknowledgment. Financial support for this research (DMR-0077321) and the purchase of a single-crystal X-ray diffractometer (CHE-9808165) from the National Science Foundation is gratefully acknowledged. The authors are in debt to Dr. M. Krawiec for his assistance with the X-ray structure analysis.

Supporting Information Available: X-ray crystallographic file, in CIF format. This material is available free of charge via the Internet at http://pubs.acs.org.

IC0342245

(15) Kunz, M.; Brown, I. D. *J. Solid State Chem.* **1995**, *115*, 395−406.
(16) The powder X-ray diffraction studies show that the cell volume decreases by 0.9% as the temperature increases from 123 to 423 K, while the largest decrease is 0.5% in *a* and increase by 0.1% in *c*.